WORLD CONFERENCE ON TIMBER ENGINEERING 2025
BRISBANE, AUSTRALIA
Advancing Timber for the Future Built Environment

INVESTIGATIONS ON ADHESIVELY BONDED TCC SPECIMENS UNDER TENSILE, CYCLIC TEMPERATURE AND SHEAR LOADING

Andreas Kirchner[1], Martin Kästner[2], Henri Paetow[3], Martin Ganß[4], Matthias Kraus[5]

ABSTRACT: To date, timber plays a minor role in the design of road bridges. However, in Germany, the traffic infrastructure is dominated by short and medium-span bridges (10 – 30 m), where adhesively bonded timber-concrete composite (ATCC) structures represent an ecologically and economically viable alternative to conventional, solid constructions. Concerning the design service life of 100 years, the long-term mechanical behavior of ATCC structures crucially depends on the durability of the adhesive joint. This contribution presents investigations on the bonding behavior, particularly the results of short-term and high-cycle fatigue compression shear tests with and without cyclic temperature preloading.

KEYWORDS: timber-concrete composite, adhesive bond, shear test, fatigue loading, temperature loading

1 – INTRODUCTION AND STATE OF THE ART

In Germany, at least 50 % of bridges in the federal highway network need a refurbishment or replacement in the next years [1]. Regarding the span widths, structures with short and medium spans (< 30 m) across waterways, roads, and railroads amount to over 50 % of bridge structures in the transportation infrastructure [2]. Steel and concrete structures dominate this big segment, with timber bridges playing only a minor role. However, regarding span widths < 30 m, timber-concrete composite (TCC) bridge superstructures represent an ecologically and economically worthwhile alternative for bridge construction [3]. In particular, the full-surface bonding of timber and concrete using adhesives offers economic and mechanical advantages compared with the punctiform or linear composite solutions used to date (e.g. stud connectors, notched or glued-in connectors). These include increased bending stiffness and reduced slip due to the rigid composite effect. Additionally, the shear load-bearing capacity of timber and concrete is better utilized. The shear load transfer into the wood is much more uniform, compared to discontinuous composite elements and a larger wood volume is activated for the shear transfer. This enables the transmission of much higher shear loads. Shorter construction times and an increase in quality due to the possibility of prefabrication in the factory when using solid or semi-finished parts for the concrete deck further emphasize the potential of adhesively bonded timber concrete structures for infrastructure construction.

The ATCC (adhesively bonded timber-concrete composite) construction method has been the subject of repeated investigations since the 1960s in various designs and can be distinguished in terms of production process (wet or dry), bonding (continuous or discontinuous), or the type of adhesive used (flexible or rigid) [4]. The short-term load-bearing behavior of ATCC components has already been investigated in several publications. Kästner [5] provides a comprehensive overview and experimental data for compression shear tests on small ATCC specimens, using different polymer mortar (hereinafter also referred to as PC – polymer concrete) types (rigid), as well as large-scale ATCC beams with continuous bond lines. Discontinuous bonding for building construction was studied experimentally and suggestions for quality control concepts were introduced by Seim and Fronmüller [6]. The “wet-on-wet” bonding process, where fresh concrete is poured on fresh adhesive, for example, was investigated amongst others in [7]. Regarding the design of TCC structures, DIN EN 1995-1-1 suggests a simplified design approach (e.g. the gamma method). Based on this method, the influence of execution type on bondline properties was investigated by Grönquist [4]. Fronmüller and Seim proposed various design methods using analytical and numerical models for ATCC structures [8].

Based on previous studies at the Bauhaus-University Weimar, the collaborative research project ‘HBVSens’ aims to establish a new construction method for TCC

[1] Andreas Kirchner, Bauhaus-University Weimar, Germany andreas.kirchner@uni-weimar.de

[2] Martin Kästner, Bauhaus-University Weimar, Germany, martin.kaestner@uni-weimar.de

[3] Henri Paetow, Bauhaus-University Weimar, Germany henri.paetow@uni-weimar.de

[4] Martin Ganß, Materials Research and Testing Institute at the Bauhaus-University Weimar, Germany, martin.ganss@mfpa.de

[5] Matthias Kraus, Bauhaus-University Weimar, Germany matthias.kraus@uni-weimar.de

https://doi.org/10.52202/080513-0093

road bridges using a highly filled, tolerance-compensating polymer mortar for continuous planar bonding between timber main girders and prefabricated concrete deck elements. As bridge constructions aim for a service life of 100 years, extensive knowledge of the durability, long-term load-bearing behavior, and fatigue behavior of the adhesive joint is required. Kästner [5] provides first experimental results regarding the cyclic loading and fatigue behavior of PC/wood and PC/concrete specimens. Long-term hygro-thermal tests under constant mechanical loading were carried out by Eisenhut [9]. However, there is little knowledge about the influence of thermal loads with high amplitudes, which may also result in stress redistributions or changes in the adhesive joint, affecting both short-term load-bearing and fatigue behavior. This study discusses the experimental results of bonded ATCC specimens under compression shear loading in quasistatic and fatigue testing, which were preloaded by a defined temperature regime. In addition to the results presented in this paper, further results of the ongoing research project 'HBVSens', including aspects related to manufacturing processes, temperature and wood moisture analyses, as well as structural health monitoring using fiber optical sensors, are presented in [10, 11, 12].

2 – PRELIMINARY INVESTIGATIONS AND ADHESION TENSILE BEHAVIOUR

The bond behavior of glued components depends strongly on the pre-treatment of the surfaces of the joining partners. In previous studies at the Bauhaus University Weimar, the bond between wood and two-component epoxy resin-based PC had already been analyzed and characterized through adhesive tensile tests [13]. The samples consisted of a wooden cube with an edge length of 100 mm and an applied mortar layer of 50 mm. Both reclaimed wood and new solid wood with rough-sawn and planed surfaces were tested. Steel plates with tabs were glued to the ends of the specimens to allow the application of force during the subsequent tests and to apply tensile stress to the joint between the wood and mortar. While a mixed fracture (fracture in the wood and near the surface of the primer) occurred in the rough-sawn surfaces, the planed samples failed 100 % in the wood.

Additional investigations on the influence of concrete surface preparations were carried out and analyzed by tensile adhesion tests based on DIN EN 1542. A total of six different concrete pretreatment combinations were investigated: formwork-smooth concrete surface (S, no pretreatment, only brushed off), sandblasted concrete surface (G), and exposed aggregate concrete surface (W), each with and without priming (V). As a primer, the unfilled resin-hardener mixture was used. For the adhesion tensile tests six concrete panels (30 x 30 x 10 cm) were manufactured with two each getting one of the aforementioned surface pretreatments (no pretreatment, sandblasting, exposed aggregate concrete). A deactivator was used to create the exposed aggregate concrete surface (type HEBAU CSE pro 70). Before applying the polymer mortar, one slab with each surface pretreatment was primed with the unfilled resin-hardener mixture. A 10 mm thin layer of polymer mortar was applied to each concrete panel. After a curing time of seven days, the samples were drilled using a core drill with a diameter of 50 mm. Deviating from the specifications of DIN EN 1542, four samples per panel were drilled to a depth of 10 mm just through the PC layer. This was done to induce adhesive failure. An additional fifth sample placed in the middle of the panel was drilled with a depth of 25 mm according to DIN EN 1542 for comparison. The corresponding test results are not considered in the following presentation of results, as these tests always resulted in tensile failure deep within the concrete.

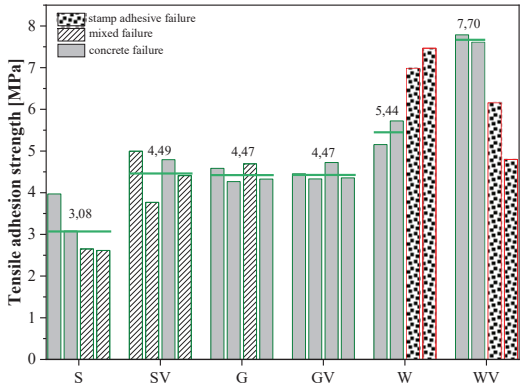

Figure 1: Results of tensile adhesion tests on PC-concrete-specimens, values over bars indicate mean values, speckled bars indicate adhesion failure between stamp and PC-surface, striped bars indicate mixed adhesion and concrete failure, gray bars indicate concrete failure, results with red outlines were excluded from the mean due to failure of the adhesive between PC-surface and stamp

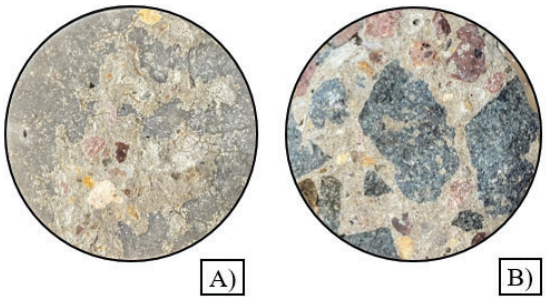

Figure 2: Typical failure surfaces in tensile adhesion tests: A) adhesion/ near surface mixed failure with formwork-smooth concrete surface, B) concrete failure in specimen with exposed aggregate concrete surface

The results of the tensile adhesion tests, i.e. maximum stresses and failure modes are shown in Fig. 1. While approximately half of all formwork-smooth samples with and without primer (S, SV) exhibited partial adhesive failure, only one of the sandblasted samples without primer (G) showed such a failure mode. Adhesive failure

https://doi.org/10.52202/080513-0093

was not observed in samples with exposed aggregate concrete surfaces (W, WV) and sandblasted samples with primer (see Fig. 2 A in comparison with Fig. 2 B). The maximum stresses of samples without adhesive failure (sandblasted primed and exposed aggregate concrete surface) range between 4.2 MPa and 7.7 MPa depending on the strength of the concrete. Adhesive failure between the PC surface and the stamp occurred for samples considering aggregate concrete surface with and without primer (bars with red borders in Fig. 1). Thus, it can be assumed that the actual tensile adhesion strength of these samples is even higher. The results confirm that the concrete surface should be profiled, to exclude adhesive failure in the concrete/PC interface. The highest load-bearing capacities and a fracture deep in the concrete were achieved with exposed aggregate concrete surfaces. Additional analyses on the polymer mortar's flow and thermomechanical behavior were conducted to ensure its usability in a realistic context [12].

3 – ATCC SPECIMEN DESIGN AND PREPARATION

The materials of the ATCC specimens for compression shear testing are spruce timber (strength class C24, ρ_{mean} = 471 kg/m³, largely knot-free) and concrete of strength class C30/37, partially C25/30. Timber parts with tangential and radial growth ring orientation were considered. The timber parts were categorized by the angle between the growth rings and the bonding surface. Subsequently, an angle between 0° and 45° is considered tangentially, and an angle between 45° and 90° is considered radially. Based on the results in section 2, concrete parts were manufactured with an exposed aggregate surface. The geometry of the specimens and the experimental setup for the compression shear tests (see Fig. 3) were selected based on studies of Zauft [14] and the recommendations of DIN EN 408. Additionally, the stiffness ratio of the concrete and wood was considered in the design process. The stiffness ratio was matched to the proposed designs of TCC bridges found by Simon [3]. The final design consisted of a 90 x 100 x 350 mm timber part and a 70 x 100 x 350 mm concrete part. The concrete and timber parts were chamfered to ensure a loading angle of 14° according to DIN EN 408. Both parts were bonded using the polymer mortar 'COMPONO S 100' consisting of a two-component epoxy resin with high mineral filler content, which is covered by a national technical approval [15]. The maximum grain size of the mineral filler measures 3.5 mm. The joint thickness was adjusted to 10 mm. To challenge failure in the joint area, the joint length was decreased to 300 mm. The joint ends run out in a circle with a radius of 5 mm to remove excessive stress accumulations. In the manufacturing process, the rounded edges were achieved using round beech timber sticks with a diameter of 10 mm.

After a minimum concrete curing time of 28 days, specimen fabrication was started. The timber parts were conditioned at 20°C and 65 % RH. Within 24 h before bonding the timber surfaces were planed and degreased with acetone. The aggregate concrete surfaces were brushed off and cleaned with compressed air.

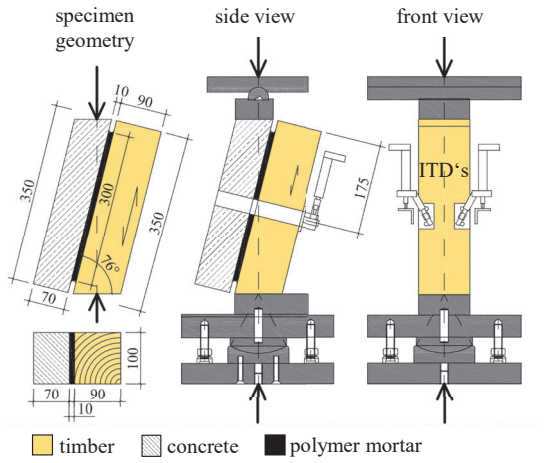

Figure 3: Specimen geometry and experimental setup

A formwork was used for the application of the polymer mortar. The timber and aggregate concrete bonding surfaces were primed with the unfilled two-component epoxy. Subsequently, polymer mortar was applied to the formed concrete parts and the timber parts were layered on top. Excessive polymer mortar was pressed out of the joint. During the fabrication of the specimens, fiber-optical strain sensors were integrated into the adhesive joint (near the wood surface). After approximately four hours, before full curing of the joint, the beech sticks were removed from the specimens. The minimum curing time before thermal preloading and/or mechanical testing was 14 days. In total 50 ATCC specimens were manufactured.

4 – EXPERIMENTAL PROCEDURE

4.1 CYCLIC TEMPERATURE PRELOADING

To investigate the effect of the cyclic fluctuation in ambient temperature associated with the seasons during the design service life of an ATCC superstructure in an accelerated manner, 26 specimens were placed in climate chambers and subjected to a predefined number of temperature cycles, modeled after EN 9142 cycle D4, as shown in Fig. 4. A temperature cycle consists of a hot and a cold phase, with heating and cooling periods in between. Aiming to include both, the maximum and minimum expected shade air temperature values for Germany (as specified in DIN EN 1991-1-5/NA:2010) within this accelerated cycle, the temperature range was set to 65 K with T_{max} = 40°C and T_{min} = -25°C. As shown in Fig. 4, both phases lasted for eleven hours. In the heating/cooling periods, the heating/cooling coefficient was aimed at roughly 1 K/min. The total time of one complete cycle lasted 24 hours. The duration of each

https://doi.org/10.52202/080513-0093

phase of one cycle was to ensure that the specimen core temperature reached the air temperature inside the chamber and was estimated through simulations and validated using preliminary tests, see Fig. 4. Due to the thermal properties of the timber, a delay in temperature between climate chamber air temperature and specimen core temperature (in the timber part) can be observed. The wood part's core temperature reached the air temperature after about five hours.

The specimens were divided into three categories and subjected to 25, 50, and 100 temperature cycles each, to simulate the effects of seasonally recurring temperature cycles over 25, 50, and 100 years, respectively. After temperature preloading, the specimens were conditioned at 20 °C and 65 % RH and subjected to quasistatic or fatigue testing according to sections 4.2 and 4.3. Temperature-induced strains were measured over the whole duration of thermal preloading on selected specimens using fiber optical sensors. The remaining 24 specimens without temperature preloading were conditioned at 20 °C and 65 % RH until testing.

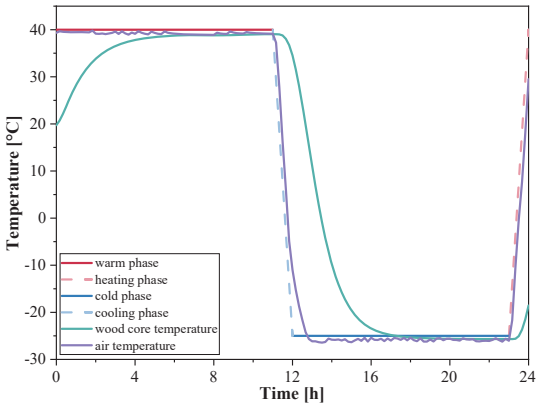

Figure 4: Modified temperature cycle based on EN 9142 cycle D4 for cyclic temperature preloading, measured climate chamber air temperature and corresponding wood core temperature measured in dummy specimen

4.2 QUASISTATIC TESTING OF ATCC SPECIMENS

Quasistatic compression shear tests using the experimental setup displayed in Fig. 3 were conducted on a total of 33 specimens. 20 of these specimens were subjected to cyclic temperature preloading as described in section 4.1. Table 1 summarizes the number of specimens with and without temperature preloading before testing.

Table 1: Summary of the experimental program

	Number of temperature cycles			
	0	**25**	**50**	**100**
Number of short-term tests	13	6	7	7
Number of fatigue tests	11	-	-	6

Tests were conducted at room temperature using a servo-hydraulic universal testing machine. The specimens were loaded displacement-controlled with a loading speed of 0.007 mm/s until failure. The force was applied with an angle of 14° relative to the specimen's longitudinal axis. Two inductive displacement transducers (IDTs) were attached to the specimens to measure the relative displacement between the concrete and wood part of the specimen in the wood fiber direction. Additionally, digital image correlation (DIC) was used to evaluate surface deformations and strains of selected specimens. Additionally, integrated fiber optical sensors were used to measure strains in the bond line for selected specimens (not discussed in this paper).

4.3 FATIGUE TESTING OF ATCC SPECIMENS

Fatigue testing based on DIN 50100 was conducted on a total of 17 ATCC specimens at room temperature. Six of these specimens were subjected to 100 temperature cycles as described in section 4.1 before fatigue testing (see Table 1).

Generally, the tests used the same experimental setup as described in section 4.2. The first fatigue test was carried out with a loading frequency of 3 Hz. As no excessive heating was observed, the loading frequency of subsequent tests was increased to 5 Hz. The sinusoidal load was applied load controlled with an R-value of 0.1 (ratio of minimum to maximum load). Quasi-static load ramps were conducted at regular intervals to monitor the development of the overall shear stiffness with an increasing number of load cycles and to potentially draw conclusions on the initiation of damage processes. The estimated maximum load F_{est} was determined based on the mean ultimate load of the first batch of quasistatic tests carried out on specimens V2 to V6. The applied maximum loads ranged from 40 % to 70 % (load levels) of F_{est} = 172.1 kN, as shown in Table 2. To prevent uneven loading, the load plate was glued to the specimens using a fast-curing two-component glue. Tests were conducted after a minimum curing time of one hour.

During the quasi-static load ramps, IDTs were used to measure the relative displacement between the concrete and the timber parts of the specimens in the wood grain direction. To ensure no excessive heating of specimens during fatigue testing, specimens were monitored using thermography. Fibre optical sensors were embedded in selected specimens to measure strain in the bond region in and perpendicular to the wood fiber direction. Additionally, DIC was used to monitor surface strain development in one specimen.

A minimum of 2 million load cycles was aimed at. To gain insight into the expected fatigue life of ATCC structures, some specimens were loaded beyond that limit without failure at one distinct load level. Once the minimum of 2 million load cycles was reached without

https://doi.org/10.52202/080513-0093

signs of failure, the specimen was labeled as runout in the present study. Staggered fatigue testing was performed on these runouts, i. e. tested again with an increased load level according to Table 2. This process was repeated until the specimen ultimately failed. In total four staggered tests were conducted. The number of failed specimens stated in Table 2 (load level ≥50%) include specimens that were tested at a lower load level before failing.

Table 2: Summary of fatigue test program and load levels, R = 0.1

Load level	F_{max} [kN]	F_{mean} [kN]	F_{min} [kN]	Number of failed specimens / (runouts)
40 %	68.5	37.7	6.9	6 / (4)
50 %	85.6	47.1	8.6	6 / (2)
60 %	102.7	56.5	10.3	4*/ (1)
70 %	119.9	66.0	12.0	1**/ (0)

** 3 specimens failed in a staggered test*
*** 1 specimen failed in a staggered test*

5 – RESULTS AND DISCUSSION

5.1 BOND BEHAVIOR UNDER QUASISTATIC LOADING

Regarding the effects of cyclic temperature preloading on the quasistatic bond behavior of the ATCC specimens, the achieved mean ultimate loads are discussed in the following. Fig. 5 compares the mean ultimate loads for the reference specimens and the specimens with cyclic temperature preloading of 25, 50, and 100 cycles. Specimens that showed manufacturing defects (see Fig. 8: specimens with < 20 % wood failure) or were suspected of having manufacturing defects (Fig. 8: specimens with a clear reduction in ultimate load and < 40 % wood failure), as well as the first specimen due to a higher loading speed, were omitted in calculating the means. The reference specimens showed a mean ultimate load of 173.7 kN.

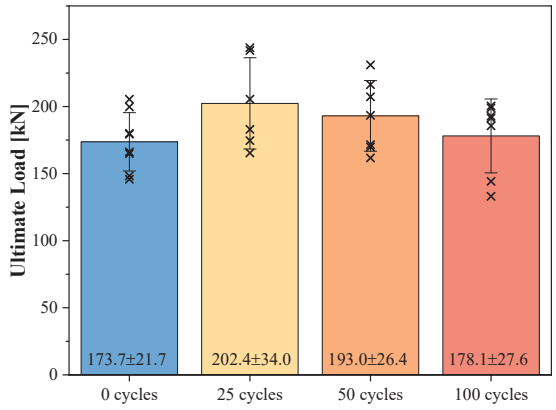

Figure 5: Mean ultimate load for ATCC specimens subjected to cyclic temperature preloading and reference specimens (0 cycles)

An overall slight increase in the mean ultimate load of the thermal preloaded specimens can be observed. The specimens preloaded with 25 temperature cycles showed a mean ultimate load of 202.4 kN. With even higher numbers of temperature cycles, the ultimate load decreased to 193.0 kN for 50 temperature cycles and 178.1 kN for 100 temperature cycles. The means of the ultimate load for specimens preloaded by cyclic temperature are higher than the means of the reference specimens in this study. Overall, no negative impact of cyclic temperature preloading on the ultimate load of the ATCC specimens was observed. The slight increase in the ultimate load of the specimens with temperature preloading migth be attributed to a post-curring of the adhesive or improvement of the interface properties between wood and adhesive. Still, the results show a high variability in the ultimate loads of the ATCC specimens. Thus, failure behaviour was further investigated.

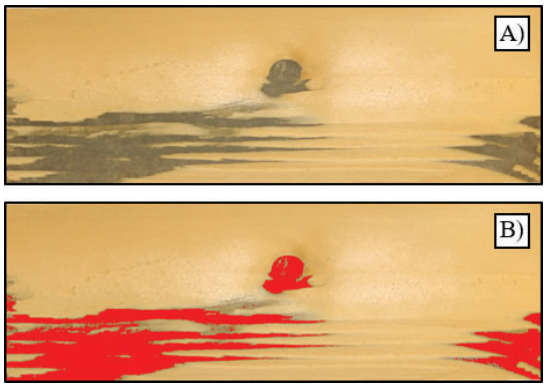

Figure 6: Example of color-based selection of the adhesive failure zone in the failure surface of an ATCC specimen for failure categorization, A) failure surface, B) color-based selection of the adhesive zone

For comparison, the failure surfaces of the specimens were analyzed. The percentage of wood failure was determined based on photos using image processing software. Color-based selection was used to determine the proportion of adhesive failure, as shown in Fig. 6. From this, the percentage of wood in the failure surface was calculated.

The observed failure modes in the ATCC specimens can be divided into three main modes: Adhesive failure in the bond line PC/wood (Fig. 7 A), cohesive failure in the wood part (Fig. 7 B), and cohesive failure in the concrete part (Fig. 7 C). Adhesive failure PC/concrete did not occur. Most specimens showed a mixed failure with parts of adhesive failure in the bond area and cohesive failure in the wooden part. Initial failure can be determined by analyzing the strain field. DIC was used to calculate corresponding strain fields from image data. Fig. 7 A to C shows examples of each main failure mode and corresponding first principal strain fields. Failure in the wood and concrete can be determined by crack formation and propagation, seen as high local pseudo-strains in the first principal stress field. Adhesive failure in the bond region shows a gradual increase in strains in the joint until sudden failure. Further, it can be observed that strains mainly accumulate in the joint region. Thus, it can

https://doi.org/10.52202/080513-0093

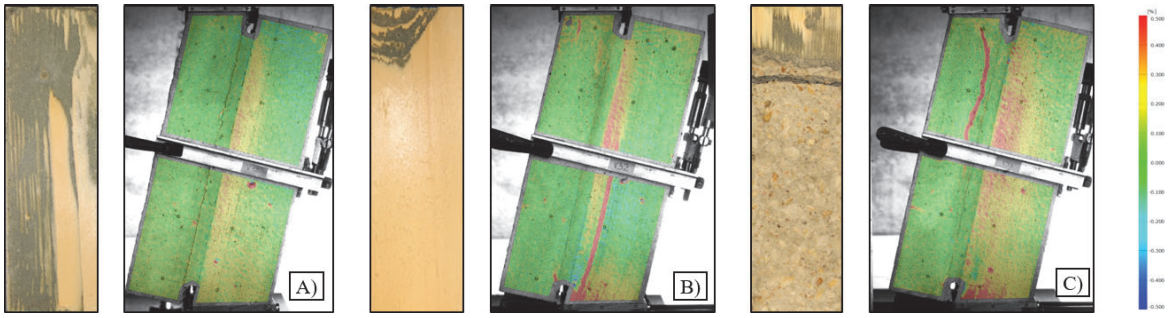

Figure 7: Failure modes in ATCC specimens in quasistatic compression shear tests and corresponding first principal strain field right before failure, captured using DIC, red indicates high strains: A) adhesive or mixed failure, B) failure in the wood part, C) failure in the concrete part

be concluded that the experimental configuration mainly causes stress in the adhesive joint.

Fig. 8 shows the ultimate load of each specimen in relation to the percentage of wood failure. The results are categorized by the growth ring orientation of the bonded timber surface, radially or tangentially, and the number of temperature cycles. Tangential specimens showed a high percentage of wood failure (> 40 %). Concrete failure only occurred in radial specimens, independent of the number of temperature cycles. Radial specimens with a wood failure percentage of less than 40 % (mostly adhesive failure) showed low ultimate loads. They were documented as having manufacturing flaws or were suspected to have such defects. Manufacturing flaws resulted from priming the wood too early before bonding or transportation of the not fully cured specimens. This probably negatively affected the chemical crosslinking at the PC/wood interface.

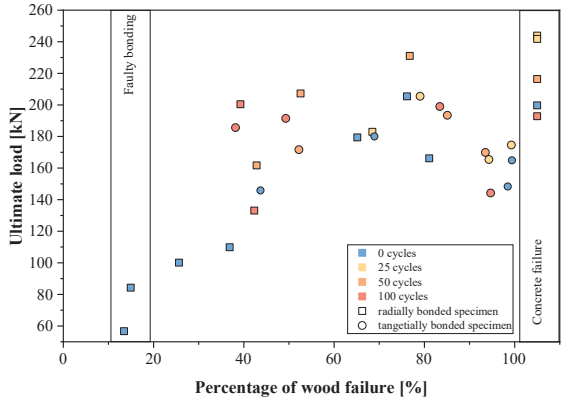

Figure 8: Ultimate load and percentage of wood in failure surface for each specimen in quasistatic testing, (color indicates the number of temperature cycles, squares indicate specimens with radially oriented wood in the bond line, circles indicate specimens with tangentially oriented wood in the bond line)

Overall, specimens exposed to cyclic temperature preloading showed a higher ultimate load. Most of these also revealed a higher percentage of wood failure exceeding 40 %. Adhesive failure (less than 20 % wood failure) occurred only in untreated specimens. Thus, it can be assumed that the temperature pretreatment had positive effects on the adhesive bonding between timber and concrete and could mitigate negative impacts resulting from manufacturing flaws.

The mean failure shear stress of all tangential specimens was calculated as 5.0 MPa. Radial specimens expressed a higher failure shear stress with 5.4 MPa, yielding a total mean of 5.2 MPa for mixed growth ring orientation. These results are in good agreement with the shear strength for defect-free spruce timber with a mixed growth ring orientation and a comparable mean density of 420 kg/m³ found in [16]. Specimens with concrete failure and radial specimens with detected or suspected manufacturing flaws were not considered in this comparative evaluation.

5.2 FATIGUE BEHAVIOR

Fig. 9 shows the load levels and the number of load cycles in fatigue testing for all tested ATCC specimens. Colors indicate failure modes according to Table 3. Runouts result from the staggered fatigue tests and are accounted for multiple times, considering each experienced load level.

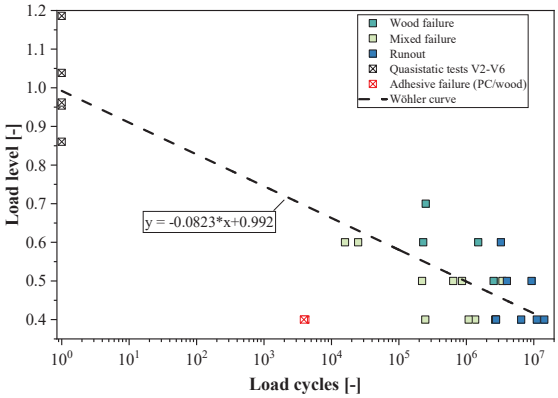

Figure 9: Load levels and reached number of load cycles for ATCC specimens in fatigue testing with compression shear loading and R = 0.1 as well as derived S-N curve (Wöhler curve), colors correspond to failure categories from Table 3.

The number of load cycles for runouts is assumed as the sum of load cycles reached at the considered load level and higher load levels. It was assumed that if a specimen was

deemed as a runout on a lower load level after X load cycles and subsequently failed at a higher load level with Y load cycles in a staggered fatigue test, the specimen could also endure (X+Y) load cycles at the lower load level. In this example, both the higher load level and Y load cycles and the lower load level and (X+Y) load cycles were considered. As some staggered tests had up to 4 stages (40 % to 70 %), this procedure was applied analogously.

Looking at individual results, a maximum of about 11 million load cycles was observed for one specimen without failure at a load level of 40 %. Two specimens only reached the minimum number of load cycles, about 4000 at a load level of 40 %. Fig. 9 clearly shows that these underperformed in relation to all other specimens. Looking at their failure modes, these specimens showed a clear adhesive failure in the PC/wood bond area. Thus, they were omitted in further analyses and the derivation of the preliminary Wöhler curve.

The S-N curve (or Wöhler curve) plotted in Fig. 9 was derived using the least squares method, considering the quasistatic test results as well. Specimens with staggered fatigue testing were accounted for each experienced load level as described beforehand. The determined S-N curve in Fig. 9 can thus be considered as an estimation on the safe side. It may be interpreted as the 50 % survival probability curve for the tested ATCC specimens. For comparison, specimens were categorized into three different failure categories by the percentage of cohesive failure in the wooden part in relation to the bonding area. Table 3 states the criteria for each category. Comparing individual results with the S-N curve shows that specimens with wood failure are above the S-N curve. Specimens with mixed failure are either on or below the S-N curve. Regarding the fatigue behavior of ATCC structures, it can be concluded that failure in the wood part results in higher fatigue resistance and thus in potentially safer and more economical structures. However, adhesive failure due to manufacturing issues must be avoided.

Table 3: Failure categories and criteria

Failure category	Percentage of wood failure in failure surface
Wood failure	> 80 %
Mixed failure	20 % … 80%
Adhesive failure	< 20 %
Concrete failure	Failure in the concrete part

Regarding the effects of cyclic temperature preloading on the fatigue behavior of ATCC specimens, no negative impact could be found. Fig. 10 shows the percentage of wood failure in relation to the number of load cycles reached at the failure load level. Specimens are distinguished by load level at failure and by the number of temperature cycles they were exposed to. A correlation between the number of endured load cycles and the percentage of wood failure is indicated. A higher percentage of wood failure correlates with an increasing number of endured load cycles. Specimens that were exposed to cyclic temperature preloading show higher numbers of endured load cycles at the same load level compared to specimens without cyclic temperature preloading. These findings show the overall positive effects of heat treatment on the mechanical behavior of ATCC structures and further emphasize the importance of preventing adhesive failure in ATCC structures.

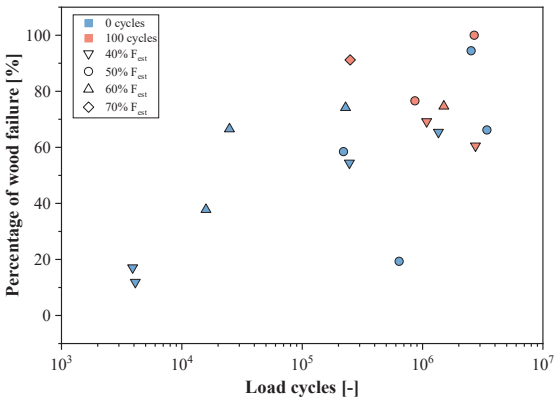

Figure 10: Percentage of wood failure and reached load cycles for each specimen in fatigue testing for failure load level (color indicates the number of temperature cycles, and the symbol indicates the failure load level)

6 – CONCLUSION AND OUTLOOK

The focus of this contribution is to investigate the effects of cyclic temperature loading on the quasistatic and fatigue behavior of ATCC specimens under compression shear loading. Preliminary tests on the tensile adhesion behavior of PC/concrete bond line for different concrete finishes show the superiority of the exposed aggregate concrete finish. This is confirmed by experimental results, as no specimen showed mixed or adhesive failur.

In quasistatic testing, no negative impact of the cyclic temperature loading on the ultimate load of ATCC specimens was found. Rather, positive effects of cyclic temperature loading were noted. Temperature-driven post-curing effects in the applied polymer mortar could be a factor leading to a slight increase in the mean ultimate load and the prevention of adhesive failure in the bonding region PC/wood.

A first Wöhler curve was derived. Comparing the individual results with the Wöhler curve confirms the findings from the quasistatic tests. Adhesive failure in the bondline PC/wood can lead to premature failure of the ATCC structure and thus should be avoided. Thermally pretreated specimens showed a higher number of endured load cycles at the same load level as untreated specimens.

Both the results of the quasistatic tests and the fatigue tests confirm that great care should be taken while manufacturing ATCC structures. A faulty bond results in adhesive failure and a greatly reduced load-bearing capacity of the structure. Temperature pretreatment could help mitigate the negative impact of faulty bonding.

https://doi.org/10.52202/080513-0093

Based on the test results, it is evident that the manufacturing process chosen for the specimens was not optimal and obviously carried a relatively high risk of adhesive failures. To address this issue, fundamental changes were made to the manufacturing process during the production of additional ATCC specimens within the ongoing research project. Several new batches of specimens were manufactured. Specimens were produced in smaller batches (4-5 specimens). Priming of the wood and concrete happened directly before bonding. As it is intended within the research project for the prefabrication of ATCC bridge superstructures in practical applications, the timber part was positioned at the bottom and the concrete element was placed on top, after the application of the polymer mortar onto the timber and concrete surface. The first results are promising. Further investigations will emphasize assessing combined cyclic temperature and mechanical shear loading.

7 – ACKNOWLEDGEMENT

Thanks go to the Fachagentur Nachwachsende Rohstoffe e.V. (FNR) and the Federal Ministry of Food and Agriculture (BMEL) of Germany for funding the ongoing research project 'HBVSens' (FNR-project no.: 2221HV097). Special thanks are extended to the industry partners Bennert GmbH, STRAB Ingenieurholzbau Hermsdorf GmbH, Beton Fertigteilbau Erfurt GmbH, HEBAU GmbH, for their support in the production of the specimens for the tensile adhesion tests and the compression shear tests. Thanks also go to the staff of the testing facility 'Versuchstechnische Einrichtung' at the Bauhaus-University Weimar and the MFPA for their support in the fabrication of the ATCC specimens and for preparation and help during testing.

8 – REFERENCES

[1] Federal Ministry for Digital and Transport (BMDV): „Brücken an Bundesfernstraßen – Bilanz und Aublick.", Bonn, 10. March 2022, https://www.bmdv.bund.de/SharedDocs/DE/Anlage/K/presse/bruecken-an-bundesfernstrassen-bilanz-und-ausblick.pdf?_blob=publicationFile, accessed on 28. March 2025.

[2] Federal Highway Research Institute (BASt): Brückenstatistik as of 01. September 2024, Bergisch Gladbach, 14. November 2024, https://www.bast.de/DE/Statistik/Bruecken/Brueckenstatistik.html, accessed on 28. March 2025.

[3] A. Simon: „Analyse zum Trag- und Verformungsverhalten von Straßenbrücken in Holz-Beton-Verbndbauweise." PhD thesis, Bauhaus-Universität Weimar, 2008.

[4] P.Grönquist, K. Müller, S. Mönch and A. Frangi: „Design of adhesively bonded timber-concrete composites: Bondline properties." conference paper, 10th International Network on Timber Engineering Research (INTER), 2023.

[5] M. Kästner: „Zum Tragverhalten von Polymermörtel-Klebverbindungen für die Anwendung bei Straßenbrücken in Holz-Beton-Verbundbauweise." PhD thesis, Bauhaus-Universität Weimar, 2019.

[6] J. Fronmüller, W. Seim, C. Umbach, J. Hummel: „Adhesively bonded timber-concrete composite construction method (ATCC) – Pilot applications in a school building in Germany." Conference paper, World Conference on Timber Engineering, Oslo, 2023.

[7] M. Breidenbach, V. Schmid, J. Wenker, C. Hein, F. Meyer, A. Dwan, K. Karbe: „Integrale Holz-Beton-Decken mit geklebtem Verbund." Research report, Technische Universität Berlin, 2022.

[8] J. Fronmüller, W. Seim: „Bond strength, failure criteria and calculation methods for adhesively bonded timber-concrete composites." In: Construction and Building Materials, April 2024.

[9] L. Eisenhut: „Geklebter Verbund aus Holz und hochfestem Beton –Untersuchungen zum Langzeitverhalten." PhD thesis, Universität Kassel, 2015.

[10] M. Ganß, A. Kirchner, M. Kästner, J. Koch, A. Simon, M. Kraus: "Investigations on ATCC components using fiber-optical sensors for structural analyses." In: Proceedings of the 5Th International Conference on Timber Bridges (ICTB 2025), Rotorua, New Zealand, 2025.

[11] J. Koch, A. Simon, M. Kästner, M. Ganß: "Analysis of the timber moisture content of an ATCC-road bridge superstructure segment." In: Proceedings of the 5Th International Conference on Timber Bridges (ICTB 2025), Rotorua, New Zealand, 2025.

[12] M. Kästner, M. Ganß, A. Kirchner, H. Paetow, J. Koch, A. Simon, M. Kraus: "Adhesively bonded timber-concrete composite structures – Analysis of thermal actions on the superstructure." In: Proceedings of the World Conference on Timber Engineering (WCTE 2025), Brisbane, Australia, 2025.

[13] K.-U. Schober: „Untersuchungen zum Tragverhalten hybrider Verbundkonstruktionen aus Polymerbeton, faserverstärkten Kunststoffen und Holz." PhD thesis, Bauhaus-Universität Weimar, 2008.

[14] D. Zauft: „Untersuchungen an geklebten Verbundkonstruktionen aus Holz und Leichtbeton.“ PhD thesis, Technische Universität Berlin, 2014.

[15] Allgemeine bauaufsichtliche Zulassung Nr. Z-10.7-282: “Polymerverguss zur Verstärkung von Holzbauteilen.” Bennert GmbH Klettbach, Deutsches Institut fuer Bautechnik, 2021.

[16] P. Glos, K. Denzler: „Kalibrierung der charakteristischen Schbfestigkeitskennwerte für Vollholz in EN 338 entsprechend dern Rahmenbedingngen der nationalen Sortiernorm“, Research report, Technische Universität München, August 2004

https://doi.org/10.52202/080513-0093